Analysis of The Semiconductor Laser Diode Using Off-axis Electron Holography and Lorentz Microscopy

Hirokazu Sasaki[*1], Shinya Otomo*[*2], Ryuichiro Minato*[*3], Junji Yoshida*[*4]*

ABSTRACT The observation of the Gallium arsenide (GaAs) model specimen and the analysis of the semiconductor laser diode were carried out by using the electron holography, which is one of the methods of the transmission electron microscope, and Lorentz microscopy. In the observation using the electron holography, not only pn junction but also interfaces which are in different dopant concentration regions of the $1x10^{19}$ and $1x10^{18}$ cm^{-3} regions and the $1x10^{18}$ and $1x10^{17}$ cm^{-3} regions could be observed. Then, the analysis example for the semiconductor laser diode was introduced and described that these methods have been used practically.

1. INTRODUCTION

In order to develop and manufacture semiconductor devices which are key components of the optical telecommunication products, such as the semiconductor laser diode, it is essential to confirm whether it is manufactured as designed. Transmission Electron Microscopy (TEM) has been used as a method to observe semiconductor devices in high magnification, and has been utilized not only in R&D but also in product management.

In case of the conventional TEM, such as a bright-field image, a dark-field image and Scanning Transmission Electron Microscopy (STEM), the information related to the orientations of the crystal, the dislocations and the atomic arrangements can be observed in the real space and then it is possible to analyze microstructures of semiconductor devices. However, in the case of these TEM, the electric potential distribution in the materials can not easily be observed. On the other hand, electric potential distributions of the semiconductor devices are designed in nanoscale, so two dimensional methods to evaluate the electrical potential in the semiconductors with a high spatial resolution are necessary for product management. Among the two dimensional electric potential distribution evaluation methods, are the Scanning Electron Microscopy (SEM)[1)], the Auger Electron Spectroscopy (AES)[2)], the Scanning Capacitance Microscopy (SCM)[3)] and the electron holography which is one method of the TEM. Here, comparison of these methods is not described here, each method is necessary to be used properly depending on its analysis purpose, in the sites of R&D and manufacturing of semiconductor devices. We have been pursuing the research for the compound semiconductor observation using the electron holography and the Lorentz microscopy, in cooperation with Nanostructures Research Laboratory in Japan Fine Ceramics Center (JFCC)[4)], and some of the results are shown in this paper.

*1 Advanced Technologies R&D Laboratories, R&D Division
*2 Corporate Planning Department, Strategy Division
*3 Telecommunications & Energy Laboratories, R&D Division
*4 Optical Devices Department, FITEL Products Division

2. SEMICONDUCTOR OBSERVATION BY ELECTRON HOLOGRAPHY AND BY LORENTZ MICROSCOPY

2.1 Electron Holography

A wave front reconstruction method from interference fringes, namely the holography, was invented by Gabor for the first time.[5)] Though he considered correcting aberration of the electron microscope using the holography, at that time it was not possible to make a highly coherent electron beam, and the holography by electron beam could not be achieved. With the subsequent development of electron gun, Tonomura et al.[6)] achieved an electron holography of one luminous flux, and the electron holography of two luminous fluxes was achieved by using an electron biprism which was invented by Möllenstedt[7)]. Then, along with the improvement of the measuring devices, remarkable research results for magnetic field observations were reported, such as the observation of magnetic field distribution in the magnetic materials and the observation of superconducting flux quantum.[8)]

In the experiments of the electron holography, the biprism is used to split the electron beam into two. (Figure 1) This is composed of a pair of ground electrodes, and a very thin conductive wire to apply voltage, which are placed in the path of the electron beam. Voltage is applied to the wire to cause the electron beam

interference by bending to attract the electron beams of both sides. The obtained interference fringe is called the hologram, and is shot with Charge Couple Device (CCD) camera and film.

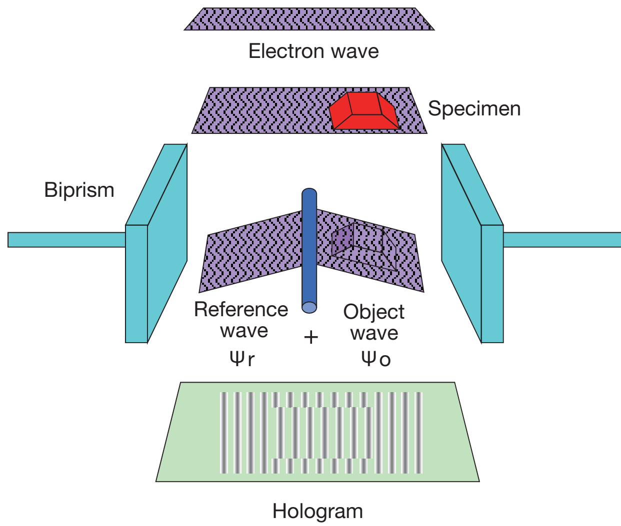

Figure 1 Schematic illustration of the electron holography.

By analyzing the interference fringe, the information of the electronic phase and amplitude can be obtained.[9] Behavior of the electron is shown by solving Schrödinger equation. In the experimental system of Figure 1, by calculating the phase change of the electronic wave function using WKB approximation, it can be expressed by the equation (1).

$$\Delta\phi=\oint_c\left(k+\frac{V}{2E}k-\frac{eA}{\hbar}\right)ds \qquad (1)$$

Here, k is a wave vector, e, $\Delta\phi$ are electron charge and phase. And $\hbar$ is a Dirac constant, E is an electronic energy, A is a vector potential, V is a scalar potential. The first term on the right-hand side represents the phase change due to the optical path difference. The second term represents the change in phase due to the electric potential. In a system where the object is placed in the electron trajectory, the term represents the internal electric potential of the object. The third term is a term associated to the vector potential A, and to the flux which is reflected. From this equation the internal electric potential change of the object placed in the electron trajectory and the flux which penetrates the surface surrounded by the electron trajectory can be observed, as the phase change of the wave function.

2.2 Semiconductor Electric Potential Distribution Observed by the Electron Holography

Electric potential in the semiconductor can be observed by using the electron holography.

Extracting only the term of the electric potential in equation (1), when the electric potential distribution in the specimen is constant for the electron transmission direction, the electric potential in the specimen can be expressed by the equation (2), as the phase difference of the electron.

$$\Delta\phi=\frac{\pi}{\lambda E}Vt \qquad (2)$$

Here, λ is the electron wavelength, E is a constant determined by the electron beam energy.

Also, t represents the specimen thickness, V represents the electric potential. From the equation (2), when the film thickness of TEM specimen is constant, we can understand that the electric potential distribution can be analyzed by detecting the phase distribution. Therefore, the preparation of a uniform TEM specimen is necessary in the semiconductor observation using the electron holography.

In 1985, Frabboni et al. in Bologna University succeeded, for the first time, in the semiconductor observation using the electron holography.[10] In their experiment, voltage was applied to the pn junction of Si, and observed the electric field generated in its surroundings. Then, the same Frabboni et al. succeeded in the observation of the electric potential distribution in the pn junction of Si to which the voltage was applied.[11] Their research was the first research that has successfully observed the electric potential change in the semiconductor by using the electron holography. Observation of the pn junction in the semiconductor, without applying voltage, was carried out by McCartney et.al.[12] They prepared the specimen by an ion milling method and a film thickness of the TEM specimen was not uniform. However, they succeeded in observing a pn junction by reducing the influence of the film thickness variation according to the correction based on the film thickness obtained from the amplitude image.

The practical observation on the semiconductor device using the electron holography was carried out by Rau et al., for the first experiment, in 1999.[13] In their observation on a Metal-Oxide-Semiconductor Field Effect Transistor (MOSFET), TEM specimen of uniform film thickness was prepared just by using mechanical polishing and Argon (Ar) milling without using the Focused Ion Beam (FIB). Then, Dunin-Borkowski et al. observed the change in the electric potential at the pn junction by applying a voltage to the TEM specimen.[14] It was Wang et al. who succeeded in the Si MOSFET observation, preparing a TEM specimen by using FIB.[15] Since the TEM specimen of a uniform thickness can be prepared in a good reproducibility by FIB, in comparison with the Ar ion-milling method, we can easily create the electric potential distribution from the phase image. Also, since the TEM specimen of a location in a specific region can be produced, a malfunction device can be selectively observed. All the above described semiconductor observation examples are related to the Si semiconductor.

We have developed the electron holography method for

the compound semiconductor, and by eliminating a FIB damaged layer[16), 17)], not only the pn junction in GaAs but also regions with different dopant concentration have been clearly distinguished.[18), 19)] In recent years, reduction of the inactive layer formed by FIB[20)], 3-dimensional observation[21)] and split-illumination electron holography[22)] have been reported. This research field has been continuing to evolve, even today.

2.3 Semiconductor Observation by the Lorentz Microscopy

The Lorentz microscopy is a method to observe the distribution of the magnetic field or the electric field using electrons deflected by the Lorentz force caused by the magnetic field and the electric field generated in the specimen. This is utilized mainly in the magnetic material analysis and a dynamic observation on magnetic flux quantum with Lorentz microscopy is the famous experimental result.[23)] Lorentz microscopy requires no special device, such as biprism which is used for the electron holography, and Fresnel method just requires defocusing during the TEM observation. Therefore, it is easy to observe in comparison with the electron holography.

Merli et al. observed a pn junction using the Lorentz microscopy, for the first time.[24)-26)] In this experiment, the TEM specimen was prepared without using FIB; clear observation was carried out, while the film thickness of the TEM specimen was not uniform.

A quantitative consideration for the Lorentz microscopy observation for the Si pn junction was discussed by Twitchett et al.[27)] As the specimens were prepared by using FIB, they tried to observe various film thicknesses of the TEM specimens. According to their experiment, in case of the Si, they concluded that the contrast of the pn junction is maximized when the film thickness of the TEM specimen is 300nm.

Then, briefly the principle of contrast generation on the Lorentz microscopy when the electrons pass though the electric field is introduced. Figure 2 is a schematic which shows electrons path through a TEM specimen with a pn junction. Due to the generated electric field in the pn junction, the electrons which pass through the specimen are deflected. Therefore, when passing through the specimen, a lot of electrons deflect and are collected to the n side, and the contrast of black and white is observed along the pn junction. In case of the over focus image, a bright line appears on the n side of the specimen and a dark line appears on the p side. In case of the under focus image, the reverse contrast from the over focus image appears.

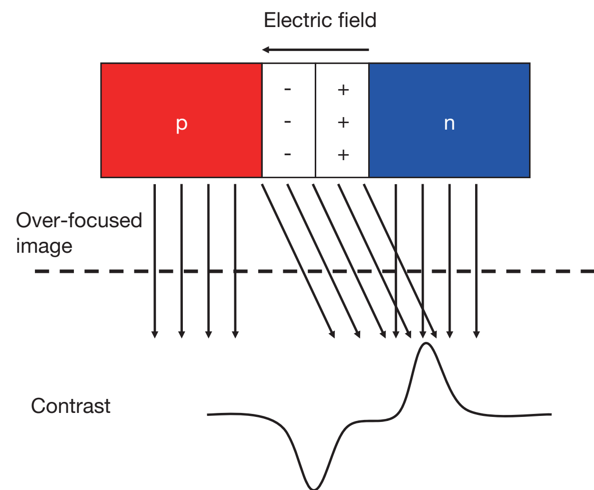

Figure 2 Schematic of the electron path through a p-n junction. (The electric field near a p-n junction deflects the electrons in one direction by Lorentz force.)

3. OBSERVATION OF THE MODEL SPECIMEN

3.1 TEM Specimen Preparation and Observation Method

As a basic experiment for utilizing the electron holography and the Lorentz microscopy in the semiconductor devices, a model specimen was prepared and a consideration of each method was carried out. The pn junctions were prepared from GaAs, and the dopant concentration was varied in each p-type region and n-type region. The variation range was from 10^{15} cm^{-3} to 10^{19} cm^{-3}, and the dopant was varied by an order of magnitude in each 200 nm of the length. Here, the used dopants were Si in the n-type region and Zinc (Zn) in the p-type region.

FIB used in the TEM specimen preparation was SMI3050TB. The final processing was performed on specimens arranged as shown in Figure 3, so that the evaluated pn junction was in parallel to the direction of the Ga ion beam. Since the slight variation of the film thickness of the TEM specimen along with the Ga ion beam direction was inevitable, by making this arrangement, a substantially uniform film thickness of the TEM specimen, towards the vertical direction of the pn junction, could be obtained. Then, the effect to vary the film thickness t, shown in the equation (2), can be reduced and the phase variation can be considered to substantially vary in proportional to the electrical potential variation. The final processing was performed to make the film thickness of the TEM specimen to 400 nm. Finally, to remove FIB damage, the Ar ion beam accelerated at 1kV was irradiated for 5 min. In the case of the arrangement shown in Figure 3, as the Ar ion beam was irradiated from the left oblique, some part of the specimen was in the shadow of the specimen holder and not milled by the Ar ion beam, and a step was formed at the boundary between the milled and unmilled parts.

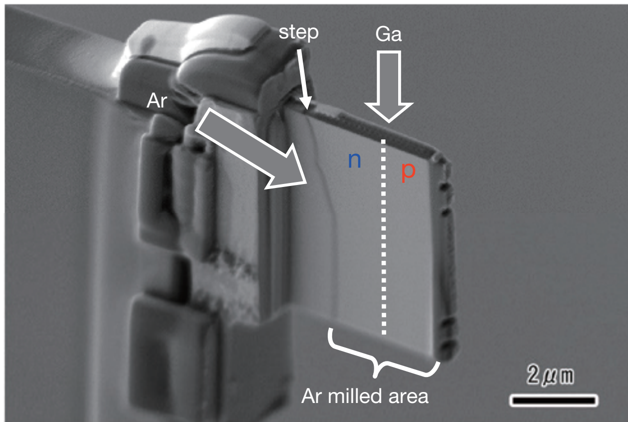

Figure 3 SEM image of the TEM specimen after the Ga ion beam and the Ar ion milling.

JEOL-3100F was used in the electron holography and in the Lorentz microscopy observation. The electron acceleration voltage was 300 kV. In the electron holography observation, 13 holograms were obtained and the phase-shifting method which had a high special resolution and a high accuracy, was used as a phase reconstruction method.[29)]

3.2 Results and Consideration

The results of superimposed intensity profiles in the Lorentz images are shown in Figure 4.

In under focus and over focus, each defocus value was photographed as 0.6 mm, 1.4 mm and 2.9 mm. The pn junction can be clearly observed in every image. On the other hand, interfaces of different dopant concentration regions can not be observed in the 0.6 mm defocus images. In the 1.4 and 2.9 mm defocused images, a contrast can be slightly observed as indicated by the arrow in Figure 4. In the n-type region, the interface between $1x10^{19}$ and $1x10^{18}$ cm^{-3} regions, and the interface between $1x10^{18}$ and $1x10^{17}$ cm^{-3} regions can be observed. In the p-type region, the interface between $1x10^{19}$ and $1x10^{18}$ cm^{-3} regions can be observed but the interface between $1x10^{18}$ and $1x10^{17}$ cm^{-3} regions can not be observed.

Figure 5 shows the electron holography phase image reconstructed by the phase-shifting method. The pn junction is clearly observed and interfaces between the multiple different dopant regions can be observed. As shown in Figure 6, the averaged phase profiles have been created to evaluate the phase image in detail. Each average phase profile for the p-type region and the n-type region are shown in Figure 6 (a) and in Figure 6 (c). In Figure 6

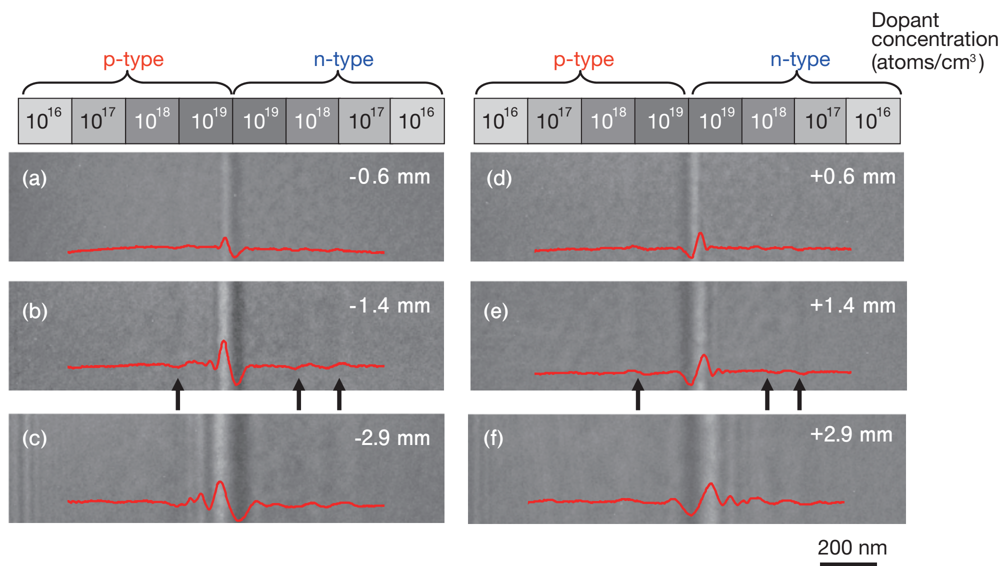

Figure 4 Observation of the GaAs with step-like dopant concentration.
(a) ~ (c) Under-focused images. (d) ~ (f) Over-focused images.

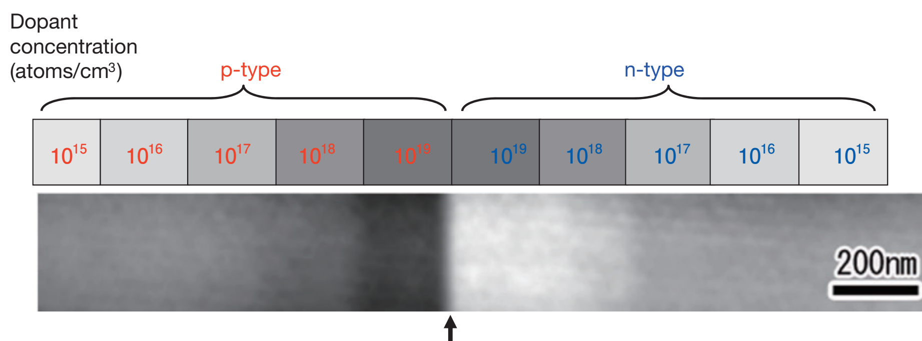

Figure 5 Phase image of the GaAs specimen reconstructed by the phase-shifting method.

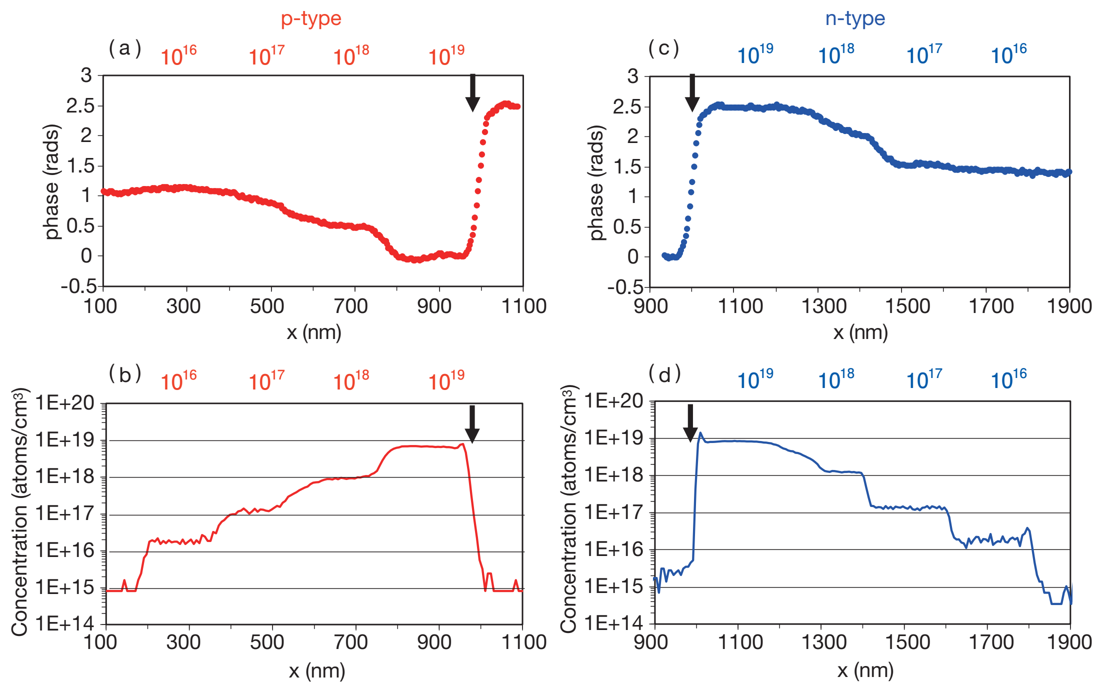

Figure 6 (a) Line profile of the phase image in the p-type region. (The arrows indicate a p-n junction.) (b) Zn SIMS profile. (c) Line profile of the phase image in the n-type region. (d) Si SIMS profile.

(b) and in Figure 6 (d), Secondary Ion Mass Spectrometry (SIMS) corresponding to the average phase profiles is shown. Figure 6 (b) shows the analysis result on the depth direction of Zn, which is a dopant, and Figure 6 (d) shows the analysis result on the depth direction of Si.

Here, from the comparison between the phase profile and the SIMS result in the p-type region, we can find that both results show the same shape of the interface profile between $1x10^{19}$ and $1x10^{18}$ cm^{-3} regions. According to the SIMS result, the interface between $1x10^{18}$ and $1x10^{17}$ cm^{-3} regions does not have a steep stepwise dopant change. Therefore, the phase profile shows a mild change. With the Lorentz microscopy, the interface between $1x10^{18}$ and $1x10^{17}$ cm^{-3} regions could not be observed. The cause was the weak electric field generated in this interface because of the non-steep electric potential change due to this mild dopant change.

Next, for the n-type region, the phase profile and the SIMS result are compared. In the phase profile, the interface between $1x10^{19}$ and $1x10^{18}$ cm^{-3} regions is not steep and the interface can not be distinguished clearly. Looking at the similar interface SIMS results, the interface is not just steep like the phase image, and is changing slowly. Thus, we can find that the phase profiles are reflecting the SIMS results. From these facts, we can understand that the electron holography can be utilized to evaluate the steepness of the interface between different dopant regions. In the phase image, the interface between $1x10^{18}$ and $1x10^{17}$ cm^{-3} regions is clear due to the steep change in dopant concentration as understood from the SIMS results. As steepness of the dopant change is high, the inter face between $1x10^{18}$ and $1x10^{17}$ cm^{-3} regions can be observed by the Lorentz microscopy, as well. In addition, the phase profile is substantially constant in the concentration regions of less than $1x10^{17}$ cm^{-3}. Depletion in the inactive layer, which is formed on the surface of the TEM specimen, and in the internal TEM specimen is thought to be the cause.

Here, the quantitative interpretation of the phase profile and the inactive layer which is formed on the surface of the TEM specimen by the FIB beam ion are discussed separately in detail in reference[28], please refer to it.[28]

4. OBSERVATION OF SEMICONDUCTOR LASER DIODE

4.1 TEM Specimen Preparation and Observation Method

The observed semiconductor laser diode had a buried structure and is prepared by Metal Organic Chemical Vapor Deposition (MOCVD). The semiconductor material was mainly composed of Indium phosphate (InP). FIB utilized for the TEM specimen preparation was SMI3050TB and the film thickness of the TEM specimen was approximately 300 nm. To remove FIB damage, an Ar ion beam accelerated by 1 kV was irradiated to the nitrogen cooled TEM specimen. HITACHI HF-3300 equipped with Cold FE electron gun was used for the electron holography and the Lorentz microscopy observation. The acceleration voltage of the electron beam was 300kV. Fourier transform method was used for the phase image reconstruction.

4.2 Observation Results

The infocus image and the defocus image observed by

the Lorentz microscopy are shown in Figure 7. The defocus value is 6.7 mm on both the under-focus image and the over-focus image. An active layer is observed in infocus image but the pn junction does not appear.

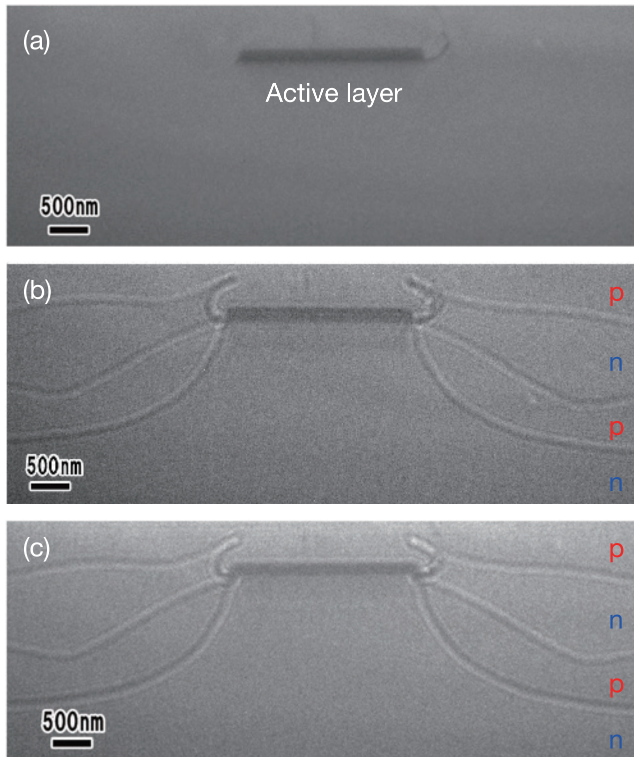

Figure 7 Observation of a semiconductor laser diode using the Lorentz microscopy.
(a) Infocus image. (b) Under-focused images. (c) Over-focused images.

Both in the under-focus image and the over-focus image, paired lines by bright lines and dark lines are clearly observed. In these two images, since the bright lines and the dark lines are inverted, then it can be understood that these lines indicate the pn junctions. Although this kind of Lorentz microscopy observation is easy, but spatial resolution is not high due to defocusing. Though pn junctions are bent in complexity on both sides of the active layer, it is not possible to make detailed observation on two dimensional distributions of fine pn junctions even if enlarged.

A phase image by the electron holography is shown in Figure 8. In Figure 8 (a), the interface region is approximately 5 μm. And the spacing between interface fringes is approximately 30 nm. Since it is reconstructed using the Fourier transform method, the spatial resolution is approximately 100 nm which is almost 3 times the fringes spacing. Similar to the Lorentz microscopy, the pn junction can be clearly observed. Also, a region of the n-type dopant present in a high concentration appears as the different contrast from the surrounding. Next, in order to observe the pn junction near the active layer in a high spatial resolution, the photograph was taken by changing the interference fringes conditions. The expanded phase image of a part of Figure 8 (a), surrounded by a dotted line, is shown in Figure 8 (b). Since the interference region is approximately 1.5 μm, and the interference fringe spacing is 5 nm, the spatial resolution is approximately 15 nm. As can be recognized from the phase image, we can understand that more detailed structure can be observed in the higher spatial resolution in comparison with the phase image in Figure 8 (a) and the Lorentz microscopy. Here, the designed location of the pn junction was positioned at the dotted line, but it was found from the electron holography observation results that the pn junction did not exist in the original position. In addition, it was found that the n-type regions each other are joined at the arrowed position. This semiconductor laser diode could not have the expected output characteristics. The structural defect of the pn junction, found out in this observation, is considered to be the cause.

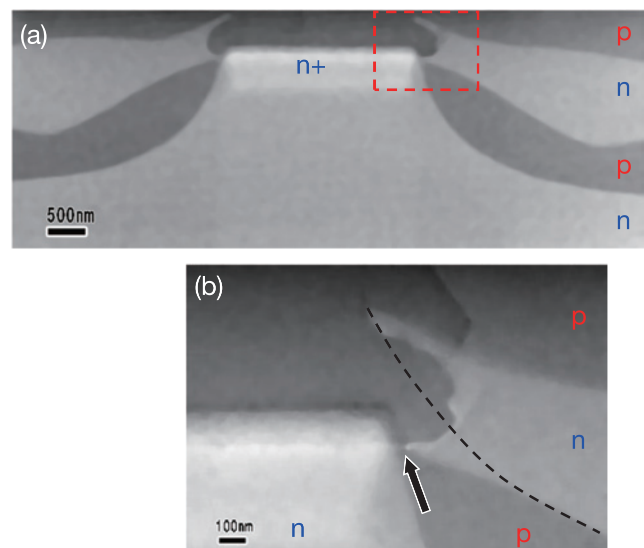

Figure 8 (a) Phase image of the semiconductor laser diode using electron holography. (b) Enlarged phase image from dashed frame in Fig. 8 (a). (Designed location of the p-n junction was at dashed line.)

5. MUTUAL COMPLEMENTARY USE OF THE ELECTRON HOLOGRAPHY AND THE LORENTZ MICROSCOPY IN SEMICONDUCTOR OBSERVATION

As described above, the electron holography and the Lorentz microscopy have advantages and disadvantages, so these are used depending on the observation purposes. The advantage of the Lorentz microscopy can be mentioned that measurements can be easily carried out as the biprism is not necessary. In addition, unlike the electron holography, a vacuum region in the vicinity of the observation field is not necessary. In case of the electron holography, presence of the reference wave passage region, in the vicinity of the observation field, is neces-

sary, and then the specimen shall be prepared by FIB so that the observation part is to be located at the edge of the TEM specimen. The issue is that, in some cases, depending on the observation device, the specimen preparation by FIB is not easy. Also, the electron holography requires selecting the appropriate interference condition, in order to obtain the expected observation region and the spatial resolution. So, in some cases, the suitable observation condition can not be prepared depending on the device. On the other hand, the Lorentz microscopy can change the magnitude appropriately by changing the excitation of the magnifying lens of the electron microscopy, similar to the conventional TEM.

The issue with the Lorentz microscopy is that the contrast can not be obtained in the weak electric field regions. For example, the low dopant concentration pn junction, the region where the dopant concentration changes gradually just like the pn junction fabricated by ion implantation and the interface with the same polarity and with slight density difference as described above, are difficult to be observed with the Lorentz microscopy. In addition, since it is the defocusing method, there is a limit to the resolution, in principle. Therefore, considering from the viewpoint of the sensitivity and the spatial resolution, the electron holography is superior. Based on these features of the two methods, in the actual device analysis, the optimum observation shall be performed by selecting one of the methods or by using both methods simultaneously.

6. CONCLUSION

In this paper, the analysis of the GaAs model specimen by the electron holography and the Lorentz microscopy were introduced. In the electron holography, the interfaces between the dopant concentration of 1×10^{19} and 1×10^{18} cm^{-3} regions, and between 1×10^{18} and 1×10^{17} cm^{-3} regions could be observed. Furthermore, the analysis examples for the semiconductor laser diode was introduced and showed that these methods are practically used.

The electron holography is a field that is still in progress and in development. By using the double-biprism method[30], the interface regions and the interface fringes can be independently varied then the observation field and the spatial resolution can be varied independently, this means that the kinds of observable device is increased. Split-illumination electron holography[22] can observe the place away from the edge of the specimen, and then the application of the devices, which were difficult to prepare specimen by FIB, becomes possible. Ultra high voltage electron holography makes possible to observe thicker the TEM specimen. Then sensitivity can be increased and there is a possibility to evaluate the lower concentricity regions of less than 1×10^{17} cm^{-3}. For other semiconductor electric voltage evaluation methods by TEM, electron diffractive imaging[31] which is one method of phase reconstruction method, Differential Phase Contrast[32] (DPC) which is one method of STEM are also effective and possible to be utilized complementarily with the electron holography. Appropriate utilization of these methods to the semiconductor device analysis can contribute to improvement of the product reliability and characteristics.

ACKNOWLEDGEMENT

At the end of the paper, we would like to thank and express our appreciation to our colleagues and contributors Dr. Tsukasa Hirayama and Dr. Kazuo Yamamoto of Nanostructures Research Laboratory in JFCC.

Furthermore, we were able to obtain a part of the achievements with the access to an apparatus of JFCC.

REFERENCES

1) F. Iwase, Y. Nakamura, and S. Furuya: "Secondary electron emission from Si-implanted GaAs", Appl. Phys. Lett., 64 (1994),
2) M. Masato, Y. Sakai, T. Ichinokawa; "Measurement and its application of the work function by scanning Auger electron microscope" J. Surf. Anal., 7 (2000), 188.
3) A. Erickson, L. Sadwick, G. Neubauer, J. Kopanski, D. Adderton and M. Rogers: "Quantitative scanning capacitance microscopy analysis of two-dimensional dopant concentrations at nanoscale dimensions", J. Electronic Materials, 25 (1996), 301.
4) General Incorporated Foundation of Japan Fine Ceramics Center; http://www.jfcc.or.jp / (Reference date November 11, 2014)
5) D. Gabor: "A new microscopic principle", Nature, 161 (1948) 777.
6) A. Tonomura, A. Fukuhara, H. Watanabe and T. Komoda:"Optical reconstruction of image from fraunhofer electron hologram", Jpn. J. Appl. Phys., 7 (1968), 295.
7) G. Möllenstedt and H. Düker: "Fresnelscher interferenzversuch mit einem biprisma für Elektronenwellen", Naturwissenschaften, 42 (1955), 41.
8) T. Matsuda, S. Hasegawa, M. Igarashi, T. Kobayashi, M. Naito, H. Kajiyama, J. Endo, N. Osakabe, and A. Tonomura:" Magnetic field observation of a single flux quantum by electron (holographic interferometry", Phys. Rev. Lett., 62 (1989), 2519.
9) E. Völkl, L. F. Allard, D. C. Joy: Introduction to Electron Holography, Kluwer Academic, Plenum Publishers, New york, (1999), 17.
10) S. Frabboni, G. Matteucci and G. Pozzi: "Electron holographic observations of the electrostatic field associated with thin reverse-biased p-n junctions", Phys. Rev. Lett., 55 (1985), 2196.
11) S. Frabboni, G. Matteucci and G. Pozzi: "Observation of electrostatic field by electron holography: the case of reversebiased p-n junctions", Ultramicroscopy, 23 (1987), 29.
12) M. R. McCartney, D. J. Smith, R. Hull, J. C. Bean, E. Voelkl and B. Frost: "Direct observation of potential distribution across Si/Si p-n junctions using off-axis electron holography", Appl. Phys. Lett., 65(1994), 2603.
13) W. D. Rau, P. Schwander, F. H. Baumann, W. Höppner, and A. Ourmazd: "Two-Dimensional Mapping of the Electrostatic Potential in Transistors by Electron Holography", Phys. Rev. Lett., 82(1999), 2614.
14) A. C. Twitchett, R. E. Dunin-Borkowski, and P. A. Midgley: "Quantitative Electron Holography of Biased Semiconductor Devices", Phys. Rev. Lett., 88 (2002), 238302.
15) Z. Wang, T. Hirayama, K. Sasaki, H. Saka and N. Kato: "Electron holographic characterization of electrostatic potential distributions in a transistor sample fabricated by focused ion beam", Appl. Phys. Lett., 80 (2002), 246.
16) K. Yabusaki, H. Sasaki "Specimen Preparation Technique for a Microstructure Analysis", Furukawa Review No.22 (September

2002)

17) H. Sasaki, T. Matusda, T. Kato. T. Muroga, Y. Iijima, T. Saitoh, F. Iwase, Y. Yamada, T. Izumi, Y. Shiohara and T. Hirayama: "Specimen preparation for high resolution transmission electron microscopy using focused ion beam and Ar ion milling", Journal of electron microscopy, 53 (2004) 497.
18) H. Sasaki, K. Yamamoto, T. Hirayama, S. Ootomo, T. Matsuda, F. Iwase, R. Nakasaki, and T. Ishii: "Mapping of dopant concentration in a GaAs semiconductor by off axis phaseshifting electron holography", Appl. Phys. Lett., 89 (2006), 244101. H.Sasaki, S.Ootomo, T. Matsuda, H. Ishii "Observation of Carrier Distribution in Compound Semiconductors Using Off-axis Electron Holography", Furukawa Review No.34 (October 2008)
20) D. Cooper, J. M. Hartmann and N. Gambacorti: "Low energy Xe milling for the quantitative profiling of active dopants by off-axis electron holography", J. Appl. Phys., 110 (2011), 044511.
21) D. Wolf, A. Lubk, A. Lenk, S. Sturm and H. Lichte:" Tomographic investigation of fermi level pinning at focused ion beam milled semiconductor surfaces", Appl. Phys. Lett., 103 (2013) 264104.
22) T. Tanigaki, S. Aizawa, H. S. Park, T. Matsuda, K. Harada and D. Shindo: "Advanced split-illumination electron holography without Fresnel fringes", Ultramicroscopy, 137 (2014) 7.
23) A. Tonomura, H. Kasai, O. Kamimura, T. Matsuda, K. Harada, Y. Nakayama, J. Shimoyama, K. Kishio, T. Hanaguri, K. Kitazawa, M. Sasase and S. Okayasu: "Observation of individual vortices trapped along columnar defects in hightemperature superconductors" Nature, 412 (2001), 620.
24) P. G. Merli, G. F. Missiroli and G. Pozzi: "Observation of p-n junction in transmission on electron microscopy by out-of-focus technique", Phys. Status Solidi (a), 16 (1973), K89.
25) P. G. Merli, G. F. Missiroli and G. Pozzi: "Contrast effects in the out-of-focus images of a p-n junction", Phys. Status Solidi (a), 20 (1973), K87.
26) P. G. Merli, G. F. Missiroli and G. Pozzi:" Transmission electron microscopy observations of p-n junctions", Phys. Status Solidi (a), 30 (1975), 699.
27) A. C. Twitchett, R. E. Dunin-Borkowski and P. A. Midgley: "Comparison of off-axis and in-line electron holography as quantitative dopant-profiling techniques", Philos. Mag. A, 86 (2006), 5805.
28) H. Sasaki, S. Otomo, R. Minato, K. Yamamoto and T Hirayama: "Direct observation of dopant distribution in GaAs compound semiconductors using phase-shifting electron holography and Lorentz microscopy" Microscopy, 63 (2014), 235.
29) K. Yamamoto, I. Kawajiri, T. Tanji, M. Hibino and T Hirayama: "High precision phase-shifting electron holography", J. Electron Microsc., 49 (2000), 31.
30) K. Harada, A. Tonomura, Y. Togawa, T. Akashi and T. Matsuda: "Double-biprism electron interferometry", Appl. Phys. Lett., 84 (2004), 3229.
31) J. Yamasaki, K. Ohta, S. Morishita and N. Tanaka: "Quantitative phase imaging of electron waves using selected-region diffraction", Appl. Phys. Lett., 101 (2012), 234105.
32) N. Shibata, S.D. Findlay, Y. Kohno, H. Sawada, Y. Kondo and Y. Ikuhara: "Differential phase-contrast microscopy at atomic resolution", Nature Phys., 8 (2012), 611.